Patterns and localized structures in population dynamics

M. G. Clerc,[1] D. Escaff,[2] and V. M. Kenkre[3]

[1]*Departamento de Física, Facultad de Ciencias Físicas y Matemáticas, Universidad de Chile, Casilla 487-3, Santiago, Chile*
[2]*Departamento de Física, Facultad de Ciencias, Universidad de Chile, Casilla 653, Santiago, Chile*
[3]*Consortium of the Americas for Interdisciplinary Science and Department of Physics and Astronomy,*
University of New Mexico, Albuquerque, New Mexico 87131, USA
(Received 6 May 2005; published 28 November 2005)

Patterns, fronts, and localized structures of a prototypical model for population dynamics interaction are studied. The physical content of the model is the coexistence of a simple random walk for the motion of the individuals with a nonlinearity in the competitive struggle for resources which simultaneously stresses the Allee effect and interaction at a distance. Mathematically, the model is variational and exhibits coexistence between different stable extended states. Solutions are obtained, the phase diagram is constructed, and the emergence of localized structures is investigated.

Population dynamics of a variety of species in nature have been successfully addressed with the help of reaction-diffusion equations [1]. The interactions among the individuals and with the environment are described by the reaction term (nonlinearity) while the transport is typically modeled by the diffusive term. Interactions with the environment are normally assumed to occur in the *immediate outskirts* of the individual, with a resulting spatially local representation. Clearly, this may not be realistic in some systems. There may be an interaction-induced modification of the environment around the individual and the elemental reaction term may therefore be more appropriately spatially nonlocal. Pattern formation resulting in such a situation which calls for the use of an integral kernel instead of a local derivative has been analyzed recently [2–4]. While that analysis will form the point of departure for our investigations in this paper, earlier [1,5,6] and later [7,8] reports of that kind of analysis are also available in the literature on the propagation of infectious diseases, firing of cells, and vegetation evolution, respectively.

Whereas the analysis of patterns given in Refs. [2–4] was based on the use of a logistic reaction-diffusion term, our present investigations assume a Nagumo term which provides an additional zero in the nonlinearity relative to the logistic case. The physical content behind such a term is the *Allee effect* [9]. Unlike in the logistic case, the zero-u solution is stable here. If u is small initially, it is attracted to the vanishing value; if large, it is attracted to the nonzero value. The physical origin of the Allee effect is the possible increase of survival fitness as a function of population size for low values of the latter. Existence of other members of the species may induce individuals to live longer whereas low densities may, through loneliness, lead to extinction. There is evidence for such an effect in nature [10]. We use the spatially nonlocal generalization of the Nagumo model here because our interest is to go beyond the simple patterns encountered in Refs. [2–4] and to analyze *localized structures* as well. Such structures have been observed in various fields: as domains in magnetic materials, chiral bubbles in liquid crystals, current filaments in gas discharge experiments, spots in chemical reactions, pulses, kinks, and localized two-dimensional states in fluid surface waves, oscillons in granular media, isolated states in thermal convection, solitary waves in nonlinear optics, and cavity solitons in lasers (see the review [11] and references therein). Localized structures are macroscopic particlelike objects, which are spatial connections between two extended steady states [12]. The most studied localized structures are *localized patterns*. These solutions are spatial connections between a homogeneous and a spatially oscillatory state [11].

In this paper we study particle-type solutions of a prototypical model for population dynamics with a nontrivial integral kernel, which we will call the variational nonlocal Nagumo model, and see that it exhibits coexistence between different stable extended states. We characterize the solutions, exhibit its phase diagram, and investigate the emergence of the localized structures.

Following the procedure in [2–4] but replacing the logistic nonlinearity by its Nagumo counterpart in a specific way leads us to

$$\partial_t u(x,t) = \partial_{xx} u + u(u-\alpha)(1-u) + u^3$$
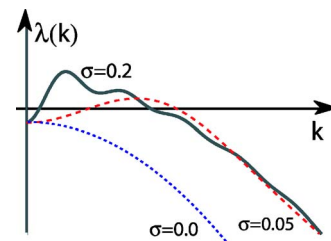$$- u(x,t) \int_\Omega u(x',t)^2 f_\sigma(x,x') d^2 x', \qquad (1)$$

FIG. 1. (Color online) Spectrum $\lambda(k)$ of the fully populated state $u(x,t)=1$, as function of the wave number k, for several values of the range of the step influence function: $\sigma=0.00$, 0.05, and 0.20.
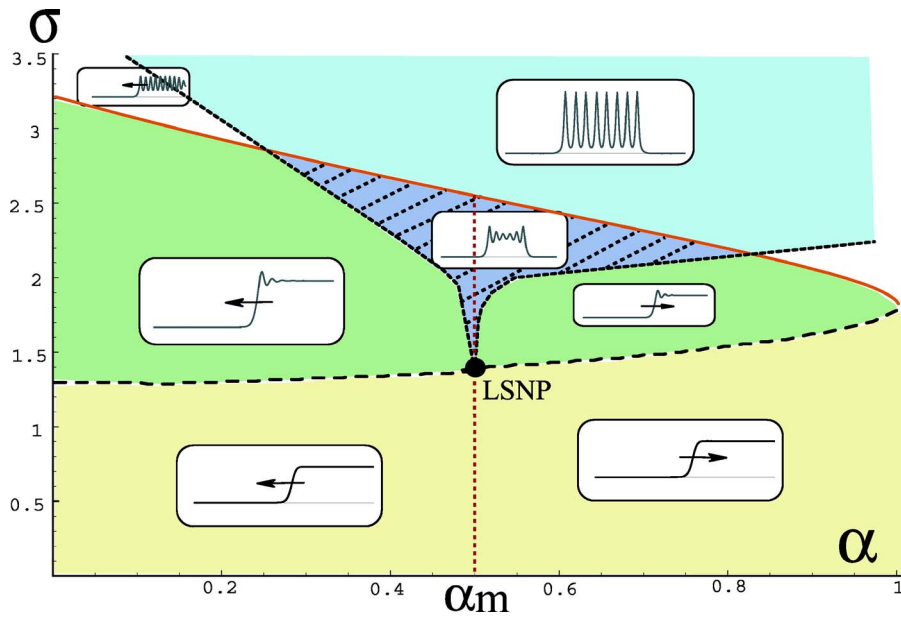
FIG. 2. (Color online) Phase diagram of our variational nonlocal Nagumo model Eq. (1) for the step influence function. The insets show representative particle-type solutions in the respective regions of parameter space. α_m represents the Maxwell point.

where $u(x,t)$ is the local density, where we have normalized all quantities in an obvious manner, and where α is a parameter that we call the *adversity*. The adversity characterizes the equilibrium point, and can always be chosen to satisfy $0 \leq \alpha \leq 1$ without loss of generality. When it is small, nonzero equilibrium population is favored. As in our previous analysis [2] we call the positive function or distribution $f_\sigma(x,x')$ the *influence function*. It is characterized by a range σ, and is normalized in the domain Ω under study. There are several ways of setting up the nonlinear spatially nonlocal term. The one we use here, as well as the case used earlier by Goldstein *et al.* [6], wherein the Fitzhugh-Nagumo evolution is treated in the limit of fast inhibitor with *linear* nonlocal term, leads to an explicitly variational problem. If, instead, one considers quadratic nonlocal terms, the system becomes non-variational and is then at once richer and more complicated to analyze [17]. We note that the nonlocal Fisher model studied in Refs. [2–4] is also nonvariational.

For simplicity, we consider the environment to be homogeneous and isotropic. Then $f_\sigma(x,x')=f_\sigma(x-x')$, with $f_\sigma(z)$ even, and $\int_\Omega f_\sigma(x,x')dx'=1$. In the extreme local limit $\sigma \to 0$, one has $f_\sigma(x,x')=\delta(x-x')$, and Eq. (1) reduces to the (local) Nagumo model. The dynamics is described by the parameters $\{\alpha,\sigma\}$ and Eq. (1) can be written as

$$\partial_t u = -\frac{\delta \mathcal{F}[u]}{\delta u}$$

where the Lyapunov functional $\mathcal{F}[u]$ has the form

$$\mathcal{F}[u] = \int_\Omega \left(\frac{1}{2}(\partial_x u)^2 + \frac{\alpha}{2}u^2 - \frac{(\alpha+1)}{3}u^3 \right) dx$$

$$+ \frac{1}{4}\int_\Omega \int_\Omega u^2 u'^2 f_\sigma(x,x')dx\, dx'.$$

Hence, the dynamics of our model (1) is of the relaxation type and the stationary states are local minima of $\mathcal{F}[u]$.

Our model (1) has three homogeneous equilibrium states: $u(x,t)=0$, 1, and α. For small σ, the steady states $\{0,1\}$ and $\{\alpha\}$ constitute stable and unstable fixed points, respectively. The steady states $u(x,t)=0$ and $u(x,t)=1$, which respectively represent the complete absence and full presence of the organism, will be termed the *unpopulated state* and *fully populated state*, respectively. The adversity α determines the global stability of the attractors and the size of their respective basin of attraction. Evaluating the Lyapunov functional in the equilibria states, one obtains $\mathcal{F}[u=0]=0$ and $\mathcal{F}[u=1]=(\alpha-1/2)\int_\Omega dx/6$. One can directly identify that the Maxwell point is $\alpha = \alpha_m \equiv 1/2$ $(\mathcal{F}[u=0]=\mathcal{F}[u=1])$. Thus, for small (large) adversity, $\alpha < \alpha_m$ $(\alpha > \alpha_m)$, the global minimum is the fully populated (unpopulated) state.

We now consider the spatial coupling and the following perturbation for the unpopulated state $u=u_0 e^{\lambda t+ikx}$, where u_0 is a small number $(u_0 \ll 1)$. We obtain the relation for the eigenvalue $\lambda(k)=-k^2-\alpha$. The eigenvalues λ are negative and decrease as functions of wave number k, and so the unpopulated state is always stable. Consequently, the nonlocal term is nonlinear and does not affect the unpopulated state. To study the stability of the fully populated state, we use an ansatz similar to the previous one, $u(x,t)=1+u_0 e^{\lambda t+ikx}$, and obtain

$$\lambda(k) = -k^2 + (\alpha+1) - 2\hat{f}_\sigma(k),$$

where $\hat{f}_\sigma$ is the Fourier transform of the influence function (compare, e.g., [4])

$$\hat{f}_\sigma(k) = \int_{-\infty}^{\infty} \cos(z)f_\sigma(z)dz.$$

Let us now consider the simple influence functions $f_\sigma(z)=\theta(\sigma+z)\theta(\sigma-z)/2\sigma$ and $f_\sigma(z)=e^{-|z|/\sigma}/2\sigma$, and $\Omega=(-\infty,+\infty)$. In these cases $\hat{f}_\sigma(k)=\sin(k\sigma)/k\sigma$ and
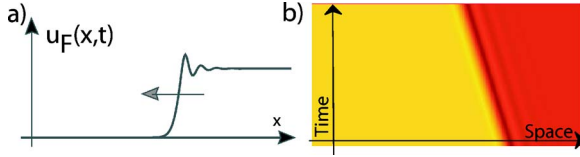
FIG. 3. (Color online) Front solution that links the fully populated state to the unpopulated state for the model in (1), for the step influence function: (a) typical front solution; (b) spatiotemporal evolution of Eq. (1), with time running upward. The intensity of the gray scale is proportional to u.
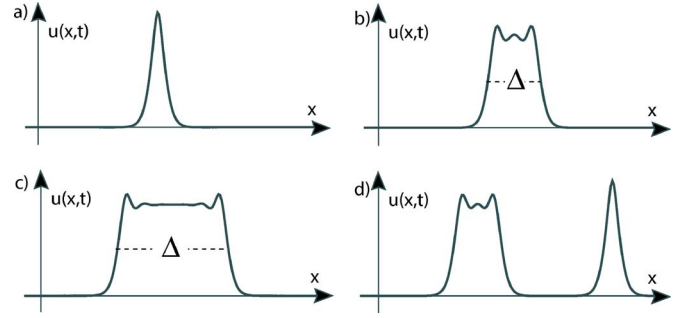

FIG. 4. (Color online) Horn solutions observed in our model (1) for the step influence function, $\alpha=0.51$, $\sigma=4\%$ of total system size, system size 250 points. (a) one-bump solution, (b) three-bump solution, (c) typical horn solution, and (d) coexistence of horn solutions. Δ is the size of the horn solution.

$\hat{f}_\sigma(k)=1/[1+(k\sigma)^2]$, respectively. When σ increases, the fully populated state becomes unstable [1]: there are some positive eigenvalues. In Fig. 1 is shown a typical spectrum of the fully populated state $[\lambda(k)]$.

The phase diagram of Eq. (1) for the step function is displayed in Fig. 2. Below the solid line, the fully populated state is stable. We have computed the solid line numerically for the step influence function but have been able to to calculate it analytically for the exponential influence function. For the latter, the explicit expression is

$$\sigma_c = \frac{\sqrt{2} + \sqrt{1-\alpha}}{1+\alpha}.$$

On this line, the homogeneous state suffers a spatial instability; above the line, the system exhibits pattern formation. The vertical dashed line represents the Maxwell manifold ($\alpha_m=1/2$). Below the solid line and $\alpha<1/2$, the fully populated state is more stable; hence if we spatially connect the fully populated state with the unpopulated state, the species invades the space at a given velocity, and we have a *front solution* [1]. In Fig. 3, we show a typical such front solution and the spatiotemporal diagram observed for (1), which illustrates the front propagation with constant speed. When α increases, $\alpha>1/2$, the population commences to disappear at a given velocity, that is, the speed of the front is reversed. At variance with the (local) Nagumo model, the front solution between the spatial homogeneous states can exhibit *spatially damped* oscillations as a consequence of the spatial nonlocality (cf. Fig. 3). Such spatially damped oscillations have been obtained from *temporal* nonlocality in the transport, i.e., from memory functions [18]. Here, the spatially damped oscillations are a consequence of the fact that for the moving reference system $[\partial_t u(x-ct)=-c\partial_x u(x-ct)]$ the fully populated state is a hyperbolic fixed point and its respective

eigenvalues have nonvanishing imaginary part. Below the horizontal dashed curve, these eigenvalues are pure real, thus the front solutions are monotonic. This dashed curve has been obtained numerically. These fronts are similar to those observed in the (local) Nagumo model ($\sigma\to0$), hence we call this region the *Nagumo zone*. For $\alpha=1/2$ and below the solid line, the front solutions that link the equilibrium states to one another are static, *wall or kink solution*.

The front solutions are particle-type solutions [12], and the interaction between them are responsible for localization (see the review [11] and references therein). In the Nagumo zone, the interaction is attractive. Thus, there are no stable localized structures there. When the wall solutions have spatially damped oscillations (cf. Fig. 3), it is well known that the nature of the kink and antikink interactions alternates between attractive and repulsive [16]. By introducing Δ the distance between the fronts (cf. Fig. 4), we see that the time dependence of Δ satisfies the law [11]

$$\dot{\Delta} = f(\Delta) \equiv \gamma \cos(\kappa\Delta)e^{-\beta\Delta} + \eta, \qquad (2)$$

where κ is the wave number and β the exponent which describe the spatially damped oscillations of the front solution [cf. Fig. 3(a)]. With the help of a specific solvability condition, in a manner similar to that explained in Ref. [11], one now obtains

$$\eta = \frac{\alpha - \alpha_m}{6\displaystyle\int_{-\infty}^{\infty} dx\, \partial_x u_F(x)^2},$$

$$\gamma = \left[\int_{-\infty}^{\infty} dx\, \partial_x u_F(x)h(x) \int_{-\infty}^{\infty} dx'\, u_F(x')^2 f_\sigma(x,x') + 2\int_{-\infty}^{\infty} dx\, u_F(x)h(x) \int_{-\infty}^{\infty} dx'\, \frac{\partial_x u_F(x')^2}{2} f_\sigma(x,x') - 3\int_{-\infty}^{\infty} dx\, \partial_x u_F(x)h(x) \right.$$
$$\left. \times \left(u_F(x) + \frac{2}{3}\right) - 2\int_{-\infty}^{\infty} dx\, h(x) \int_{-\infty}^{\infty} dx'\, \partial_x u_F(x')f_\sigma(x,x') \right] \bigg/ \int_{-\infty}^{\infty} dx\, \partial_x u_F(x)^2,$$
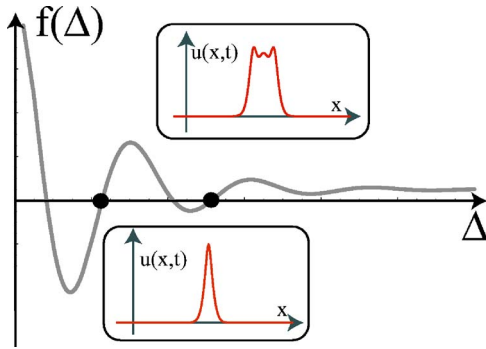
FIG. 5. (Color online) Oscillatory interaction force $f(\Delta)$. The inset figures are the stable localized patterns observed close to the Maxwell point. The extent of these localized patterns is marked by circles.

where $u_F(x)$ is the front solution with damped oscillations of model (1), $h(x)$ being the function $\cos(\kappa x)e^{-\beta x}$. In Fig. 3(a), we show the characteristic front solution under analysis.

From this kink and antikink interaction Eq. (2), one deduces that the system exhibits different localized states and the size of these solutions Δ^* satisfy $\cos(\kappa\Delta^*)\exp(-\beta\Delta^*) = -\eta/\gamma$. In Fig. 5 are illustrated the the kink interaction and the steady state of Eq. (2).We term these steady states *horn solutions*. In Fig. 4 we show such horn solutions observed in Eq. (1). Their lengths are approximately multiples of the shortest localized state length, which is related to the characteristic length κ of the spatially damped oscillations.

We have determined, both numerically and analytically, the point in the parameter space where the horn solutions appear for the two kinds of influence function we have analyzed: step and exponential, respectively. For the exponential influence function this point is $\alpha=1/2$ and $\sigma=\sqrt{2/3}$. We term this point the *localized structures nascent point* (LSNP) and denote it in Fig. 2 by LSNP. In the parameter space, the horn solutions appear and disappear around the LSNP by saddle-node bifurcations. The smallest horn solution is stable inside the dashed zone (cf. Fig. 2). This zone has been determined numerically for both the step and exponential influence functions. The other horn solutions have a similar region of stability inside the dashed zone and all these regions have vertices in the LSNP.

Above the solid line in Fig. 2, the fully populated state suffers a spatial instability and gives rise to the appearance of patterns. A typical such pattern is shown in Fig. 6(a). In this parameter region the system has coexistence between a spatially homogeneous state and a spatially periodic one, a *periodic population state*. One can understand the appearance of these patterns as being a self-organization response of the population to the large range of the competition interactions function and the surrounding adversity.

As result of spontaneous breaking of spatial symmetry, a front solution between the unpopulated state and periodic population one, it is motionless in a range of parameters called the pinning range [13]. This phenomenon is well known as the locking phenomenon [13]. One can consider the interaction of two fronts and obtain a similar expression to (2) amended with a periodic term [14]. One then sees that the front interaction alternates between being attractive and repulsive. Hence, one can find an infinite number of localized structures, which we will call *localized patterns* [14]. In Figs. 6(c) and 6(d) are shown such localized patterns observed from Eq. (1). They are above the solid line and inside the dotted curve.

Recently, static localized patterns have been studied from the point of view of their geometrical existence [15]. The localized patterns appear and disappear close to the pinning range. The different localized patterns appear and disappear by saddle-node bifurcation and they have a geometrical sequence of bifurcations around the pinning range [14,15].

Numerically, we have computed the zone where the shortest localized pattern, i.e., the localized state with fewer bumps, is stable. This zone corresponds to the inside of the dotted line and above the solid line in Fig. 2. Above the solid line (small α) and outside the dotted line, the periodical equilibrium state always invades the unpopulated one with a well defined velocity.

In summary, we have studied the fronts and localized structures of a prototypical model for population dynamics with a nontrivial influence function for the spatially nonlocal competition interactions and found the system to exhibit a coexistence between different stable extended states. We have characterized the different particle-type solutions and presented their phase diagram. We have also determined and characterized the point in the phase space where the localized structures appear, the *localized structure nascent point*. Our theory should be of interest for a wide variety of phenomena, not only in biological systems, in which context the
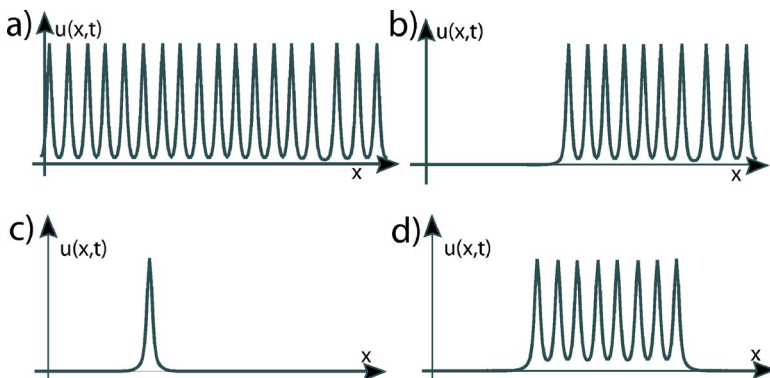

FIG. 6. (Color online) Pattern, front solution, and localized patterns observed from our model (1) for $\alpha=0.618$, $\sigma=4\%$ of total system size, system size 250 points. (a) Periodic solution, (b) front solution that links the unpopulated state and the periodic fully populated state, (c) first-bump localized pattern, and (d) eighth-bump solutions.

applications are obvious, but also in sociological systems in which the formation of localized structures that emerge naturally from the model we use might correspond to localized clusters of communities with similar opinions or ideological approach. Work on such applications is under way.

The simulation software DIMX developed by P. Coullet and collaborators at the laboratory INLN in France has been

[1] J. D. Murray, *Mathematical Biology* (Springer-Verlag, Berlin, 1989).

[2] M. A. Fuentes, M. N. Kuperman, and V. M. Kenkre, Phys. Rev. Lett. **91**, 158104 (2003).

[3] V. M. Kenkre, in *Modern Challenges in Statistical Mechanics: Patterns, Noise, and the Interplay of Nonlinearity and Complexity*, edited by V. M. Kenkre and K. Lindenberg, AIP Conf. Proc. No. 658 (AIP, Melville, 2003).

[4] M. A. Fuentes, M. N. Kuperman, and V. M. Kenkre, J. Phys. Chem. B **108**, 10505 (2004).

[5] D. G. Kendall, *Mathematics and Computer Science in Biology and Medicine* (Medical Research Council, London, 1965).

[6] R. E. Goldstein, D. J. Muraki, and D. M. Petrich, Phys. Rev. E **53**, 3933 (1996).

[7] E. Hernandez-Garcia and C. Lopez, Phys. Rev. E **70**, 016216 (2004); C. Lopez and E. Hernandez-Garcia, Physica D **199**, 223 (2004).

[8] E. Gilad, J. von Hardenberg, A. Provenzale, M. Shachak, and E. Meron, Phys. Rev. Lett. **93**, 098105 (2004).

[9] W. C. Allee, *The Social Life of Animals* (Beacon Press, Boston, 1938).

[10] F. Courchamp, T. Clutton-Brock, and B. Grenfell, Trends Ecol. Evol. **14**, 405 (1999); P.A. Stephens and W. J. Sunderland, *ibid.* **14**, 401 (1999); C. W. Fowler and J. D. Baker, Rep. Int. Whal. Comm. **41**, 545 (1999).

[11] P. Coullet, Int. J. Bifurcation Chaos Appl. Sci. Eng. **12**, 245 (2002).

[12] M. C. Cross and P. C. Hohenberg, Rev. Mod. Phys. **65**, 851 (1993).

[13] Y. Pomeau, Physica D **23**, 3 (1986).

[14] M. G. Clerc and C. Falcon, Physica A **356**, 48 (2005).

[15] P. Coullet, C. Riera, and C. Tresser, Phys. Rev. Lett. **84**, 3069 (2002).

[16] P. Coullet, C. Elphick, and D. Repaux, Phys. Rev. Lett. **58**, 431 (1987).

[17] M. G. Clerc, D. Escaff, and V. M. Kenkre (unpublished).

[18] K. K. Manne, A. J. Hurd, and V. M. Kenkre, Phys. Rev. E **61**, 4177 (2000).